

Importance of voltage-dependent inactivation in N-type calcium channel regulation by G-proteins

Norbert Weiss · Abir Tadmouri · Mohamad Mikati · Michel Ronjat · Michel De Waard

Received: 9 October 2006 / Accepted: 29 October 2006 / Published online: 14 December 2006
© Springer-Verlag 2006

Abstract Direct regulation of N-type calcium channels by G-proteins is essential to control neuronal excitability and neurotransmitter release. Binding of the $G_{\beta\gamma}$ dimer directly onto the channel is characterized by a marked current inhibition (“ON” effect), whereas the pore opening- and time-dependent dissociation of this complex from the channel produce a characteristic set of biophysical modifications (“OFF” effects). Although G-protein dissociation is linked to channel opening, the contribution of channel inactivation to G-protein regulation has been poorly studied. Here, the role of channel inactivation was assessed by examining time-dependent G-protein de-inhibition of $Ca_v2.2$ channels in the presence of various inactivation-altering β subunit constructs. G-protein activation was produced via μ -opioid receptor activation using the DAMGO agonist. Whereas the “ON” effect of G-protein regulation is independent of the type of β subunit, the “OFF” effects were critically affected by channel inactivation. Channel inactivation acts as a synergistic factor to

channel activation for the speed of G-protein dissociation. However, fast inactivating channels also reduce the temporal window of opportunity for G-protein dissociation, resulting in a reduced extent of current recovery, whereas slow inactivating channels undergo a far more complete recovery from inhibition. Taken together, these results provide novel insights on the role of channel inactivation in N-type channel regulation by G-proteins and contribute to the understanding of the physiological consequence of channel inactivation in the modulation of synaptic activity by G-protein coupled receptors.

Keywords N-type calcium channel · $Ca_v2.2$ subunit · G-protein · G-protein coupled receptor · μ -opioid receptor · inactivation · β subunit

Abbreviations

GI	G-protein inhibition
GPCR	G-protein coupled receptor
DAMGO	(D-Ala ² ,Me-Phe ⁴ ,glycinol ⁵)-enkephalin
rMOR	rat μ -opioid receptor
PCR	polymerase chain reaction
RI	recovery from inhibition
NS	non-statistically significant

N. Weiss · A. Tadmouri · M. Ronjat · M. De Waard (✉)
Laboratoire Canaux Calciques, Fonctions et Pathologies,
Inserm U607, CEA,
17 rue des Martyrs,
38054 Grenoble Cedex 09, France
e-mail: michel.de-waard@cea.fr

M. Mikati
Department of Pediatrics,
American University of Beirut Medical Center,
Beirut, Lebanon

N. Weiss · A. Tadmouri · M. Ronjat · M. De Waard
Commissariat à l’Energie Atomique,
Grenoble, France

N. Weiss · A. Tadmouri · M. Ronjat · M. De Waard
Université Joseph Fourier,
Grenoble, France

Introduction

Voltage-dependent N-type calcium channels play a crucial role in neurotransmitter release at the central and peripheral synapse [3, 47]. Several subtypes of N-type channels, which differ in their inactivation properties either because of differences in subunit composition [43] or because they represent splice variants [5, 28], are known to exist. N-type

channels are strongly regulated by G-protein coupled receptors (GPCR) [4, 18, 25, 29, 30]. Direct regulation by G-proteins involves the binding of the $G_{\beta\gamma}$ dimer [22, 27] on various structural determinants of $Ca_v2.2$, the pore-forming subunit of N-type channels [1, 11, 15, 23, 34, 38, 44, 53]. This regulation is characterized by typical biophysical modifications of channel properties [16], including (1) a marked current inhibition [7, 51], (2) a slowing of activation kinetics [30], (3) a depolarizing shift of the voltage-dependence of activation [4], (4) a current facilitation after prepulse depolarization [26, 42], and (5) a modification of inactivation kinetics [52]. Current inhibition has been attributed to $G_{\beta\gamma}$ binding onto the channel (“ON” effect), whereas all other channel modifications are a consequence of a variable time-dependent dissociation of $G_{\beta\gamma}$ from the channel (“OFF” effects) [49]. Although the dissociation of $G_{\beta\gamma}$ was previously described as voltage-dependent [17], it was then suggested that channel opening after membrane depolarization was more likely responsible for the removal of $G_{\beta\gamma}$ [35]. More recently, we have shown that the voltage-dependence of the time constant of $G_{\beta\gamma}$ dissociation was directly correlated to the voltage-dependence of channel activation suggesting that $G_{\beta\gamma}$ dissociation is in fact intrinsically voltage-independent [49].

Although $G_{\beta\gamma}$ dissociation, and the resultant characteristic biophysical changes associated with it, has been correlated with channel activation, the contribution of channel inactivation in G-protein regulation has been barely studied. Evidence that such a link may exist has emerged from a pioneering study from the group of Prof. Catterall [23] in which it was demonstrated that mutations of the β -subunit binding domain of $Ca_v2.1$, known to affect inactivation, also modifies G-protein modulation. A slower inactivating channel, in which the Arg residue of the QQIER motif of this domain was substituted by Glu, enhanced the prepulse facilitation suggesting that the extent of G-protein dissociation was enhanced. However, establishing a specific relationship between channel inactivation and G-protein regulation with mutants of such a motif is rendered difficult because this motif is also a $G_{\beta\gamma}$ -binding determinant [15, 23, 53]. Indeed, mutations of this motif are expected to decrease the affinity of G-proteins for the channel and, hence, may facilitate G-protein dissociation. Differences in G-protein regulation of $Ca_v2.2$ channels have also been reported if the channel is associated to β subunit that induces different inactivation kinetics [12, 20, 31]. However, a formal link between channel inactivation and G-protein regulation was not established in any of these studies.

In this study, we analyzed how modifying channel inactivation kinetics could affect the parameters of G-protein dissociation (time constant and extent of dissociation). We used a method of analysis that was recently

developed on N-type channels for extracting all parameters of G-protein regulation at regular potential values, independently of the use of prepulse depolarizations [48]. The objective was to perform a study in which the structural properties of the pore-forming subunit would remain unaltered to keep the known G-protein binding determinants of the channel functionally intact. Structural analogues of β subunits, known or expected to modify channel inactivation properties, were used [14, 32, 40]. It is concluded that fast inactivation accelerates G-protein dissociation from the channel, whereas slow inactivation slows down the process. However, channel inactivation also reduces the temporal window of opportunity in which G-protein dissociation can be observed. Far less recovery is observed for channels that undergo fast inactivation, whereas slow inactivating channels display almost complete G-protein dissociation. With regard to the landmark effects of G-protein regulation, it is concluded that the “ON” effect (extent of G-protein inhibition) is independent of the type of inactivation provided by β subunits, whereas all “OFF” effects (slowing of activation and inactivation kinetics, shift of the voltage-dependence of activation) are largely influenced by the kinetics of channel inactivation induced by the β constructs. These results better explain the major differences that can be observed in the regulation of functionally distinct N-type channels. Furthermore, they provide an insight of the potential influence of channel inactivation in modulating G-protein regulation of N-type channels at the synaptic level.

Materials and methods

Materials

The cDNAs used in this study were rabbit $Ca_v2.2$ (GenBank accession number D14157), rat β_{1b} (X61394), rat β_{2a} (M80545), rat β_3 (M88751), rat β_4 (L02315), and rat μ -opioid receptor (rMOR, provided by Dr. Charnet). (D-Ala²,Me-Phe⁴,glycinol⁵)-enkephalin (DAMGO) was from Bachem (Bubendorf, Germany).

Molecular biology

The CD8- β_{1b} chimera was generated by polymerase chain reaction (PCR) amplification of the full-length β_{1b} using oligonucleotide primers 5'-CGCGGATCCGTCCAGAA GAGCGGCATGTCCCGGGGCCCTTACCCA-3' (forward) and 5'-ACGTGAATTCGCGGATGTAGACGCC TTGTCCCAGCCCTCCAG-3' (reverse), and the PCR product was subcloned into the *Bam*HI and *Eco*RI sites of the pcDNA3-CD8- β ARK-myc vector after removing the β ARK insert (vector generously provided by D. Lang,

Geneva University, Geneva, Switzerland). The truncated N-terminal β_{1b} construct ($\beta_{1b \Delta N}$, coding for amino acid residues 58 to 597) was performed as described above using the primers 5'-CGCGGATCCACCATGGGCTCAGCAGAGTCTACACGAGCCGGCCGTCAGAC-3' (forward) and 5'-CGGGGTACCGCGGATGTAGACGCCTTGTCACAGCCCTCCAGCTC-3' (reverse), and the PCR product was subcloned into the *KpnI* and *BamHI* sites of the pcDNA3.1(-) vector (Invitrogen). The truncated N-terminal β_3 construct ($\beta_3 \Delta N$, coding for amino acid residues 16 to 484) was performed using the primers 5'-CGCGGATCCACCATGGGTTTCAGCCGACTCCTACACCAGCCGCCCTCTCTGGAC-3' (forward) and 5'-CGGGGTACCGTAGCTGTCTTTAGGCCAAGGCCGGTTACGCTGCCAGTT-3' (reverse), and the PCR product was subcloned into the *KpnI* and *BamHI* sites of the pcDNA3.1(-) vector.

Transient expression in *Xenopus* oocytes

Stage V and VI oocytes were surgically removed from anesthetized adult *Xenopus laevis* and treated for 2–3 h with 2 mg/ml collagenase type 1A (Sigma). Injection into the cytoplasm of cells was performed with 46 nl of various cRNA mixture in vitro transcribed using the SP6 or T7 m Message mMachine Kit (Ambion, Cambridgeshire, UK; 0.3 $\mu\text{g}/\mu\text{l}$ $\text{Ca}_v2.2+0.3 \mu\text{g}/\mu\text{l}$ μ -opioid receptor+0.1 $\mu\text{g}/\mu\text{l}$ of one of the different calcium channel β constructs). Cells were incubated at 19°C in defined nutrient oocyte medium as described [19].

Electrophysiological recording

After incubation for 2–4 days, macroscopic currents were recorded at room temperature (22–24°C) using a two-electrode voltage-clamp in a bathing medium containing (in millimolar): $\text{Ba}(\text{OH})_2$ 40, NaOH 50, KCl 3, HEPES 10, niflumic acid 0.5, pH 7.4 with methanesulfonic acid. Electrodes filled with (in millimolar) KCl 140, EGTA 10, and HEPES 10 (pH 7.2) had resistances between 0.5 and 1 M Ω . Macroscopic currents were recorded using Digidata 1322A and GeneClamp 500B amplifier (Axon Instruments, Union City, CA). Acquisition and analyses were performed using the pClamp 8 software (Axon Instruments). Recordings were filtered at 2 kHz. Leak current subtraction was performed on-line by a P/4 procedure. DAMGO was applied at 10 μM by superfusion of the cells at 1 ml/min. All recordings were performed within 1 min after DAMGO produced maximal current inhibition. We observed that this procedure fully minimized voltage-independent G-protein regulation that took place later, about 5–10 min after DAMGO application (data not shown). Hence, the inhibition by DAMGO was fully reversible as assessed by washout

experiments. Also, no rundown was observed during the time course of these experiments. Cells that presented signs of prepulse facilitation before μ -opioid receptor activation (tonic inhibition) were discarded from the analyses.

Analyses of the parameters of G-protein regulation

The method used to extract all biophysical parameters of G-protein regulation (GI_{t_0} , the initial extent of G-protein inhibition before the start of depolarization, τ , the time constant of G-protein unbinding from the channel, and RI, the extent of recovery from inhibition at the end of a 500-ms test pulse, unless specified in the text) were described elsewhere [48]. The key steps required to extract these parameters are briefly summarized in Fig. 1. This method is analogous to the method that relies on the use of prepulses but avoids many of the pitfalls of the latter (use of an interpulse potential that favors G-protein re-association, differences in the rate of channel inactivation between control and G-protein regulated channels, and facilitation that occurs during the control test pulse) [48].

Mathematical and statistical analyses

Current–voltage relationships (I/V) were fitted with the modified Boltzmann equation $I_{(V)} = (G_{\text{max}} \times (V - E)) / (1 + \exp(-(V - V_{1/2})/k))$ where $I_{(V)}$ represents the maximal current amplitude in response to a depolarization at the potential V , G_{max} is the maximal conductance, E is the inversion potential of the Ba^{2+} , and k is a slope factor. All data are given as mean \pm SEM for n number observations and statistical significance (p) was calculated using Student's t test. Statistical significance for scatter plot analysis was performed using the Spearman rank order correlation test.

Results

N-type current inhibition by G-proteins is independent of the β subunit species

G-protein inhibition is generally studied through the measurement of the peak currents. However, this approach does not take into account the fact that, at the time to peak, a considerable proportion of G-proteins has already dissociated from the channel during depolarization. To better estimate the real extent of N-type current inhibition by G-proteins, we used the technical approach described in Fig. 1 to measure GI_{t_0} , the maximum extent of G-protein inhibition before the start of the G-protein unbinding process. Representative current inhibition and kinetic alterations are shown for $\text{Ca}_v2.2$ channels co-expressed with the β_{1b} , β_{2a} , β_3 , or β_4 subunit (Fig. 2a, top panel) and

the corresponding GI_{t_0} values were quantified (Fig. 2a, bottom panel). The β subunits did not alter significantly the maximum extents of inhibition that ranged between $59.2 \pm 1.4\%$ ($Ca_v2.2/\beta_{2a}$ channels, $n=25$) and $62.4 \pm 1.8\%$ ($Ca_v2.2/\beta_{1b}$ channels, $n=25$; Fig. 2b). In the following part of this study, three other β subunit constructs have been co-expressed with $Ca_v2.2$, $\beta_{1b \Delta N}$, $CD8-\beta_{1b}$, and $\beta_3 \Delta N$. As for the wild-type β isoforms, GI_{t_0} varied not significantly ($p > 0.05$) between $58.4 \pm 1.8\%$ ($\beta_{1b \Delta N}$, $n=9$) and $63.5 \pm 1.3\%$ ($CD8-\beta_{1b}$, $n=10$).

The two parameters that are relevant for the “OFF” effects, τ (the time constant of G-protein unbinding from the channel), and RI (the extent of current recovery from G-protein inhibition after a 500-ms depolarization) will be used to investigate the role of N-type channel inactivation in G-protein regulation. GI_{t_0} is not a time-dependent parameter and cannot be influenced by the time course of inactivation.

Current recovery from G-protein inhibition is altered when the inactivation kinetics of $Ca_v2.2$ channels are modulated by β subunits

Auxiliary β subunits are known to influence the inactivation kinetics of $Ca_v2.2$ channels with a rank order of potency, from the fastest to the slowest, of $\beta_3 \geq \beta_4 > \beta_{1b} \gg \beta_{2a}$ [45]. Representative control current traces at 10 mV for $Ca_v2.2$ channels co-expressed with each type of β subunit are shown in Fig. 3a (left panel). As expected from former reports, the β_3 subunit produces the fastest inactivation, whereas β_{2a} induced the slowest inactivation. The β_{1b} and β_4 subunits induce intermediate inactivation kinetics. In agreement with previous reports [12, 20], β subunits markedly affect G-protein regulation. Here, we investigated how channel inactivation affects the kinetics of G-protein departure from the channel and the extent RI. The time constants τ of G-protein dissociation were extracted from the $I_{G-proteins \text{ unbinding}}$ traces for each combination of channels (Fig. 3a, middle panel), whereas RI was calculated as the extent of dissociation by comparing the current levels of I_{DAMGO} , $I_{DAMGO \text{ wo unbinding}}$, and $I_{Control}$ after 500 ms of depolarization (Fig. 3a, right panel). The data show that both τ and RI values are differentially affected by the kinetics of channel inactivation. Average parameters are reported in Fig. 3b (for τ) and Fig. 3c (for RI). The time constant τ of recovery from G-protein inhibition is 2.9-fold faster for the fastest inactivating channel ($Ca_v2.2/\beta_3$, 37.5 ± 3.3 ms, $n=13$) than the slowest inactivating channel ($Ca_v2.2/\beta_{2a}$, 107.8 ± 2.7 ms, $n=22$). Interestingly, the rank order for the speed of recovery from G-protein inhibition ($\beta_3 \geq \beta_4 > \beta_{1b} \gg \beta_{2a}$) is similar to that observed for inactivation kinetics. Indeed, Student's *t* tests demonstrate that differences between β subunits are all

highly statistically significant ($p \leq 0.001$) except between β_3 and β_4 where the difference is less pronounced ($p \leq 0.05$; Fig. 3b). Thus, it is concluded that the speed of channel inactivation imposed by each type of β subunit impacts the time constant of recovery from G-protein inhibition. Channel inactivation appears as a “synergistic factor” to channel activation [49] for the speed of G-protein dissociation. Next, the effects of β subunits were investigated on RI values (Fig. 3c). Two of the β subunits (β_3 and β_4) have closely related RI values ($56.9 \pm 1.8\%$ ($n=21$) vs $56.8 \pm 1.2\%$ ($n=34$)). In contrast, β_{1b} and β_{2a} statistically decrease ($45.0 \pm 1.3\%$, $n=24$) and increase ($96.1 \pm 1.4\%$, $n=29$) RI values, respectively. From these data, it is clear that faster recovery from inhibition is not necessarily associated with an elevated RI value. Although channel inactivation accelerates the kinetics of G-protein dissociation from the channel, it also reduces the time window in which the process can be completed. In these data, a relationship seems to exist between channel inactivation conferred by β subunits and G-protein dissociation. However, it is unclear whether this link is only due to the kinetics of inactivation conferred by β subunits or also to differences in molecular identities. In order to precisely assess this first observation, we examined how structural modifications of individual β subunits, known to alter channel inactivation, affect the recovery parameters from G-protein inhibition.

Deletion of a β subunit determinant important for fast inactivation alters recovery from G-protein inhibition

Important determinants for the control of inactivation rate have been identified in the past on β subunits [32, 37]. Deletion of the amino terminus of β subunits is known to slow down channel inactivation [14]. According to the data of Fig. 3, slowing of inactivation should increase both the time constant τ of recovery from G-protein inhibition and the extent of RI. Figure 4a,b illustrates the extent of slowing in inactivation kinetics of $Ca_v2.2/\beta_{1b}$ channels when the first 57 amino acids of β_{1b} subunit at the N-terminus are deleted ($\beta_{1b \Delta N}$). The amount of inactivation at the end of a 500-ms depolarization at 10 mV shows a 2.2-fold decrease from $58.4 \pm 1.6\%$ ($n=22$) to $26.2 \pm 2.3\%$ ($n=10$; Fig. 4b). Representative traces of DAMGO regulation of $Ca_v2.2/\beta_{1b}$ and $Ca_v2.2/\beta_{1b \Delta N}$ currents demonstrate that the deletion of the N terminus of β_{1b} produces a significant modification in G-protein regulation (Fig. 4c, left panel). Notably, DAMGO-inhibited $Ca_v2.2/\beta_{1b \Delta N}$ currents display much slower activation kinetics (quantified in Fig. 8c). The analysis of the time course of $I_{G-proteins \text{ unbinding}}$ traces in the presence of truncated β_{1b} reveals a slower time course (Fig. 4c, middle panel). Also, the deletion of the N terminus of β_{1b} leads to an increased recovery from G-protein inhibition (Fig. 4c, right panel). Statistical analyses

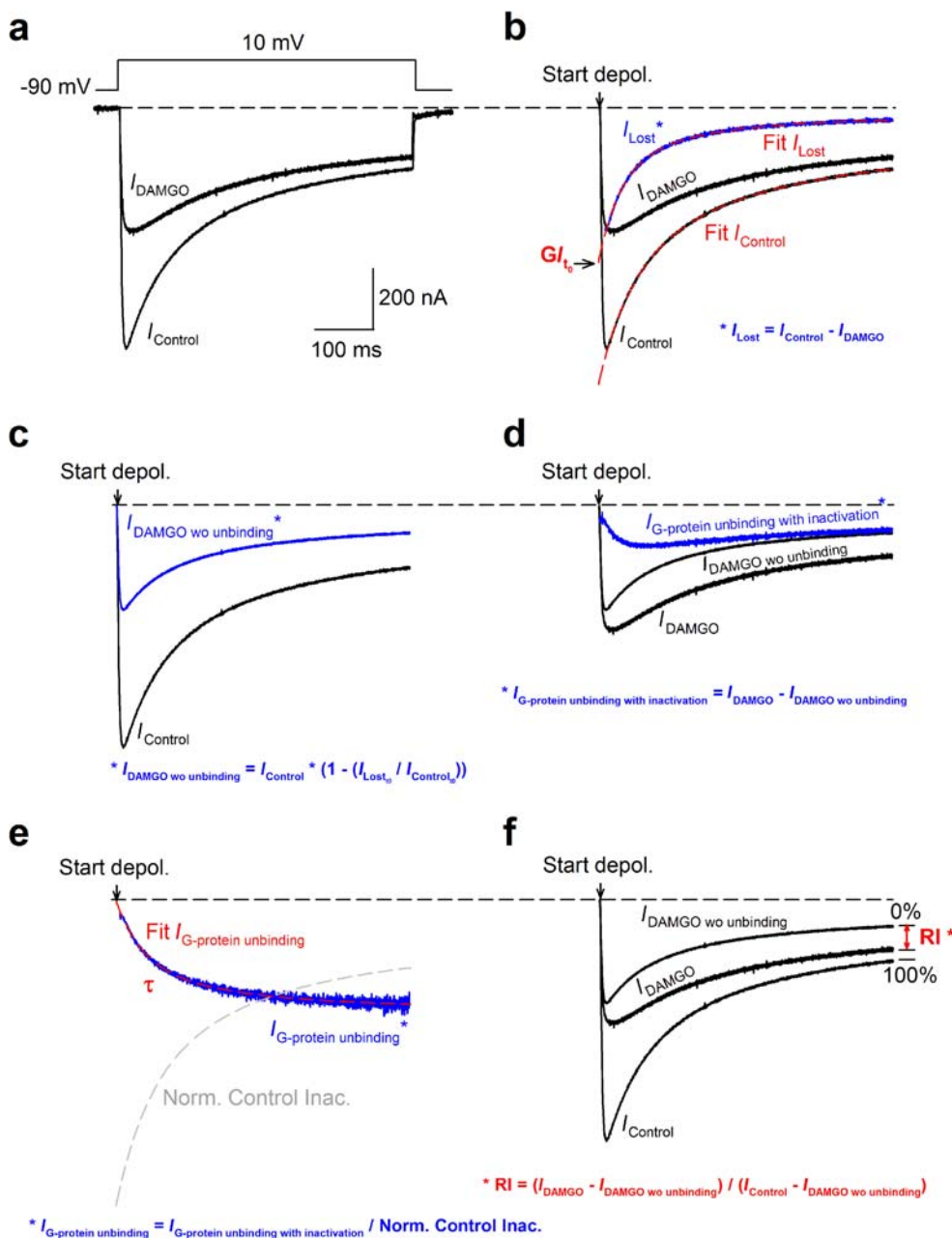


Fig. 1 Illustration of steps leading to the determination of the biophysical parameters of N-type currents regulation by G-proteins according to [48]. **a** Representative $\text{Ca}_v2.2/\beta_3$ current traces elicited at 10 mV for control (I_{Control}) and DAMGO (I_{DAMGO}) conditions. **b** Subtracting I_{DAMGO} from I_{Control} results in I_{Lost} (blue trace), the evolution of the lost current under G-protein activation. I_{Control} and I_{Lost} are then extrapolated to $t=0$ ms (the start of the depolarization) by fitting traces (red dashed lines) with a single and double exponential, respectively, to determine GI_{t_0} , the maximal extent of G-protein inhibition. **c** I_{DAMGO} without unbinding ($I_{\text{DAMGO wo unbinding}}$, blue trace) represents an estimate of the amount of control current that is present in I_{DAMGO} and is obtained by the following equation: $I_{\text{DAMGO without unbinding}} = I_{\text{Control}} \times \left(1 - \left(I_{\text{Lost}_0} / I_{\text{Control}_0}\right)\right)$. **d** Subtracting

$I_{\text{DAMGO wo unbinding}}$ from I_{DAMGO} results in $I_{\text{G-protein unbinding with inactivation}}$ (blue trace), the evolution of inhibited current that recovers from G-protein inhibition after depolarization. **e** $I_{\text{G-protein unbinding with inactivation}}$ is divided by the fit trace (normalized to 1) describing inactivation kinetics of the control current (gray dashed line) to reveal the net kinetics of G-protein dissociation ($I_{\text{G-protein unbinding}}$, blue trace) from the channels. A fit of $I_{\text{G-protein unbinding}}$ by a mono-exponential decrease provides the time constant τ of G-protein dissociation from the channel. **f** The percentage of recovery from G-protein inhibition (RI, in red) at the end of 500 ms pulse is measured as $RI = (I_{\text{DAMGO}} - I_{\text{DAMGO wo unbinding}}) / (I_{\text{Control}} - I_{\text{DAMGO wo unbinding}}) \times 100$. Arrows indicate the start of the depolarization

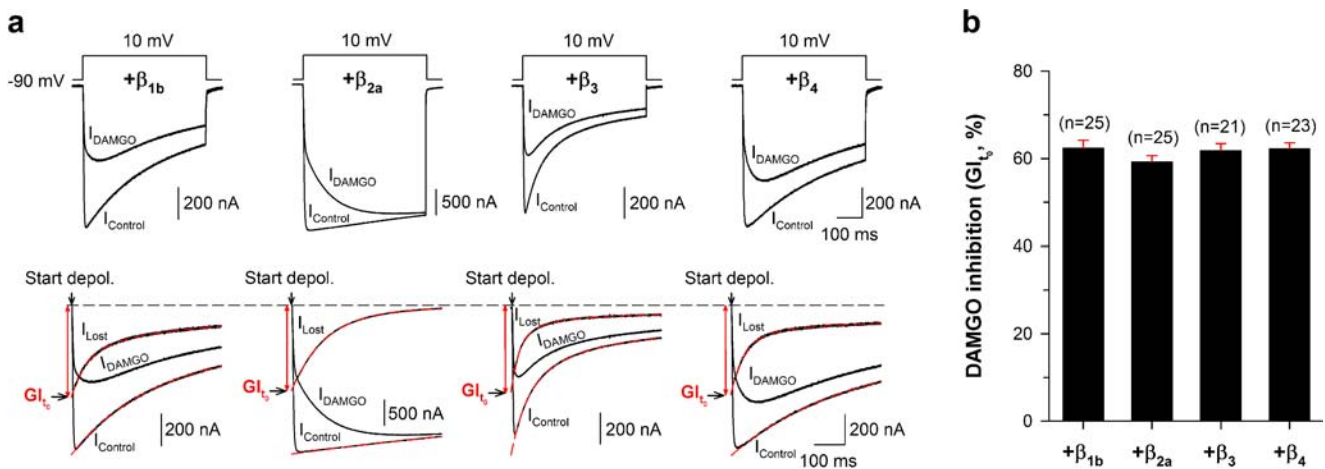


Fig. 2 Maximal G-protein inhibition of N-type currents is independent of the type of β subunits. **a** Representative current traces elicited at 10 mV before (I_{Control}) and under 10 μM DAMGO application (I_{DAMGO}) for $\text{Ca}_v2.2$ channels co-expressed with the β_{1b} , β_{2a} , β_3 , or β_4 subunit (top panel). Corresponding traces allowing the measurement of the maximal DAMGO inhibition at the start of the depolarization (GI_t) are also shown for each experimental condition (bottom panel). I_{Control} and I_{Lost} (obtained by subtracting I_{DAMGO} from I_{Control}) were

fitted by a mono- and a double exponential, respectively (red dashed lines), to better estimate the maximal extent of DAMGO-inhibited current before the start of the depolarization (GI_0). The red double arrow indicates the extent the DAMGO-inhibited current at $t=0$ ms. Traces were normalized at the maximal value of I_{Control} at $t=0$ ms to easily compare the extent of current inhibition. **b** Block diagram representation of GI_0 for each experimental condition. Data are expressed as mean \pm SEM (in red) for n studied cells

show a significant increase in the time constant τ of recovery (2.0-fold) from 60.0 ± 2.0 ms ($n=24$) to 118.6 ± 2.5 ms ($n=10$; Fig. 4d) and an increase in the RI values (1.8-fold) from $45.0 \pm 1.3\%$ ($n=24$) to $79.6 \pm 2.5\%$ ($n=9$) by the deletion of the N terminus of β_{1b} (Fig. 4e).

To confirm that these effects are independent of the nature of the β subunit involved, similar experiments were conducted with a 15-amino acid N-terminal truncated β_3 subunit $\beta_{3\Delta\text{N}}$. As for $\beta_{1b\Delta\text{N}}$, $\beta_{3\Delta\text{N}}$ produces a slowing of channel inactivation kinetics. After 500 ms at 10 mV, $\text{Ca}_v2.2/\beta_3$ channels inactivate by $68.9 \pm 1.7\%$ ($n=21$) compared to $41.1 \pm 1.1\%$ ($n=10$) for $\text{Ca}_v2.2/\beta_{3\Delta\text{N}}$ channels (Fig. 5a,b). As expected, DAMGO inhibition of $\text{Ca}_v2.2/\beta_{3\Delta\text{N}}$ channels produces currents with slower activation and inactivation kinetics than $\text{Ca}_v2.2/\beta_3$ channels (shift of the time to peak of the current from 20.7 ± 2.5 ms with β_3 ($n=21$) to 77.0 ± 7.6 ms with $\beta_{3\Delta\text{N}}$ ($n=10$); Fig. 5c, left panel). Moreover, the time course of $I_{\text{G-proteins}}$ unbinding was slowed down with the N-terminal truncation of β_3 (Fig. 5c, middle panel), and the recovery from inhibition was enhanced (Fig. 5c, right panel). Quantification of these effects reveals a statistically significant slowing (1.8-fold) of the time constant of recovery τ from G-protein inhibition from 37.5 ± 3.3 ms ($n=13$) to 67.4 ± 4.5 ms ($n=10$; see Fig. 5d) and an increase of RI values (1.2-fold) from $56.9 \pm 1.8\%$ ($n=21$) to $66.9 \pm 2.1\%$ ($n=10$; see Fig. 5e). However, the time constant of recovery in the presence of $\beta_{3\Delta\text{N}}$ remains fast compared to the inactivation kinetics, which

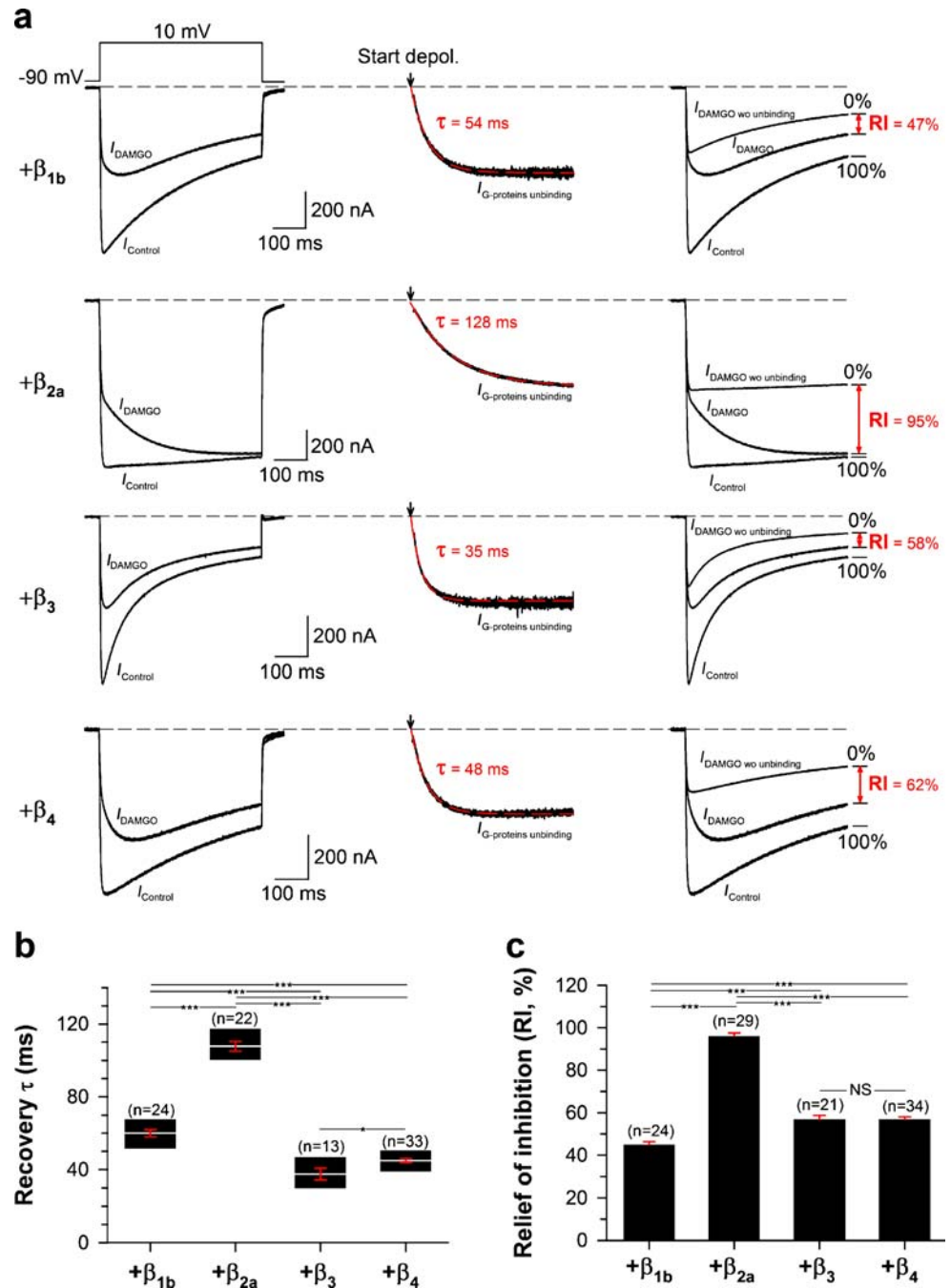
may explain the lower increase in RI values compared to what has been measured with $\beta_{1b\Delta\text{N}}$. Also, the starting value of RI is high for β_3 (56.9%) compared to β_{1b} (45.0%), which limits the possibility of increase.

Slowing of channel inactivation by membrane anchoring of β subunit also alters the properties of recovery from G-protein inhibition

Another approach to modulate channel inactivation is to modify the docking of the β subunits to the plasma membrane [13, 40]. For that purpose, we expressed a membrane-inserted CD8 linked to the β_{1b} subunit (CD8- β_{1b}) along with $\text{Ca}_v2.2$. As shown in earlier studies using the same strategy but with a different β subunit [2, 40], membrane anchoring of the β_{1b} subunit significantly slows down the inactivation kinetics (Fig. 6a). Indeed, inactivation was reduced by 1.5-fold from $58.4 \pm 1.6\%$ ($n=22$) to $38.1 \pm 1.8\%$ ($n=10$; see Fig. 6b). Membrane anchoring of β_{1b} via CD8 slowed down the DAMGO-inhibited current activation kinetics (Fig. 6c, left panel). Under DAMGO inhibition, a greater shift of the time to peak of the current was observed for CD8- β_{1b} than for β_{1b} (from 57.0 ± 4.1 ms with β_{1b} ($n=12$) to 168.8 ± 7.0 ms with CD8- β_{1b} ($n=10$)). Also, recovery from inhibition was slowed 1.9-fold from 60.0 ± 2.0 ms ($n=24$) to 112.3 ± 5.4 ms ($n=8$; Fig. 6d), whereas RI increased 1.3-fold from $45.0 \pm 1.3\%$ ($n=24$) to $58.0 \pm 1.9\%$ ($n=9$; see Fig. 6e).

Fig. 3 Influence of β subunits on the recovery of N-type channel inhibition by G-proteins.

a Representative current traces before ($I_{Control}$) and during application of 10 μ M DAMGO (I_{DAMGO}) are shown at 10 mV for $Ca_v2.2$ channels expressed with β_{1a} , β_{2a} , β_3 , or β_4 subunit (left panel). Corresponding $I_{G-protein\ unbinding}$ traces are shown for each condition (middle panel) and were fitted by a mono-exponential decrease (red dashed line) to determine the time constant τ of G-protein unbinding from the channel. The arrow indicates the start of the depolarization. Traces that allowed the measurement of RI values (in red) are also shown for each condition (right panel). **b** Box plot representation of the time constant τ of G-protein unbinding as a function of the type of β subunit co-expressed with $Ca_v2.2$ channels. The number of cells studied is indicated in parentheses. **c** Block diagram representation of RI values measured after 500 ms depolarization as a function of the type of the β subunit expressed with $Ca_v2.2$ channels. Data are expressed as mean \pm SEM (in red) for n studied cells. Statistical t test: NS not statistically significant, single asterisk $p \leq 0.05$, two asterisks $p \leq 0.01$, three asterisks $p \leq 0.001$

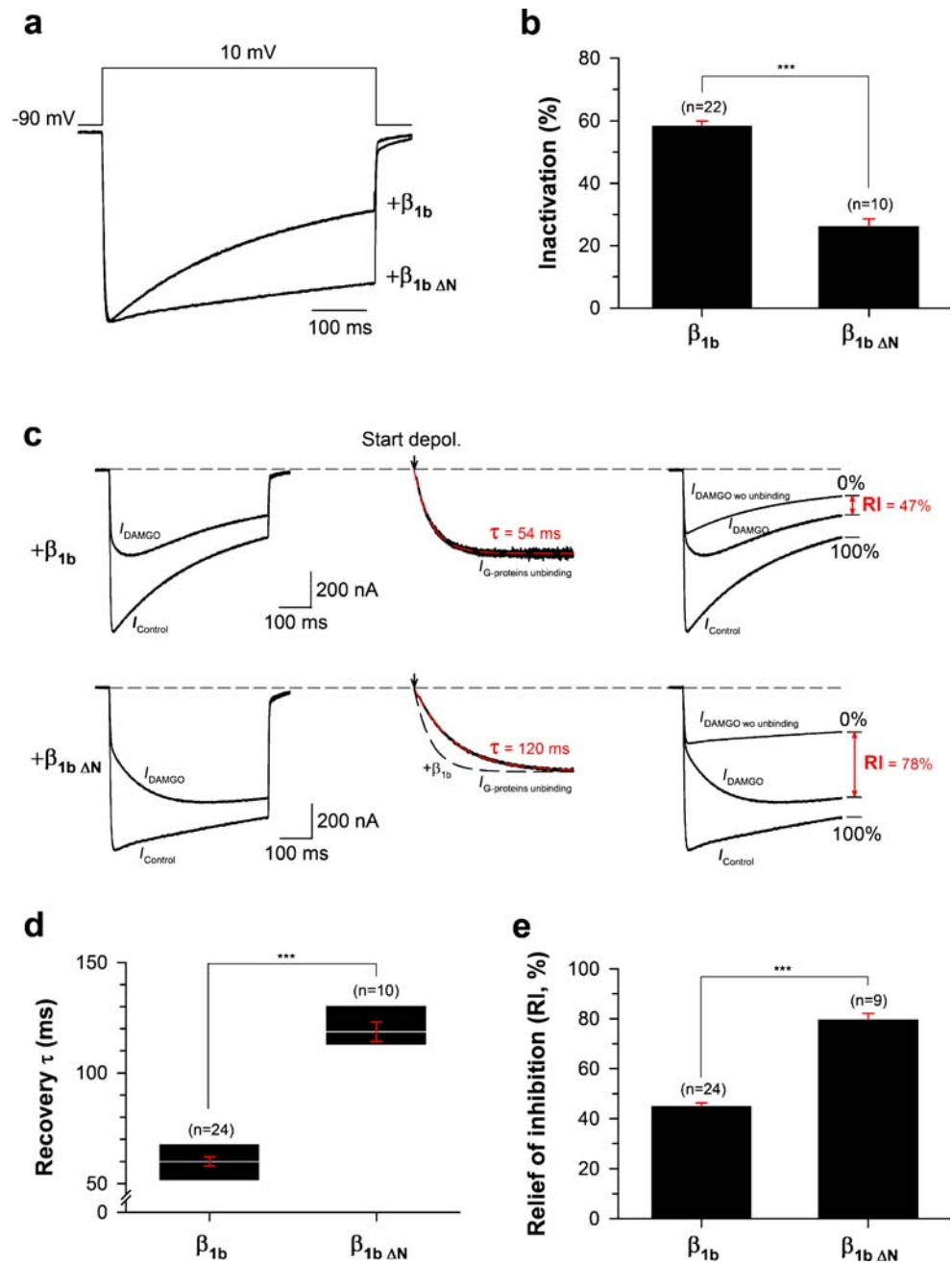


Inactivation limits the maximum observable recovery from G-protein inhibition

As demonstrated above, inactivation influences both the time constant of recovery and the maximal observable recovery from inhibition. To study the effect of channel inactivation on the maximum recovery from inhibition independently of the time constant of recovery, we compared RI values and inactivation at a fixed time constant of recovery. The time constant of recovery from inhibition shows a voltage

dependence similar to that of channel opening [49]. An example of this voltage dependence is illustrated in Fig. 7a (left panel) for $Ca_v2.2/\beta_{1b}$ channels. A plot of the time constant of recovery as a function of membrane depolarization indicates a great extent of variation in τ values (Fig. 7a, middle panel). This voltage dependency of τ values was observed for all channel combinations (data not shown). We then chose to impose the τ value to 50 ± 5 ms for all expressed channel combinations by selecting the appropriate recordings from the set of traces obtained at various test

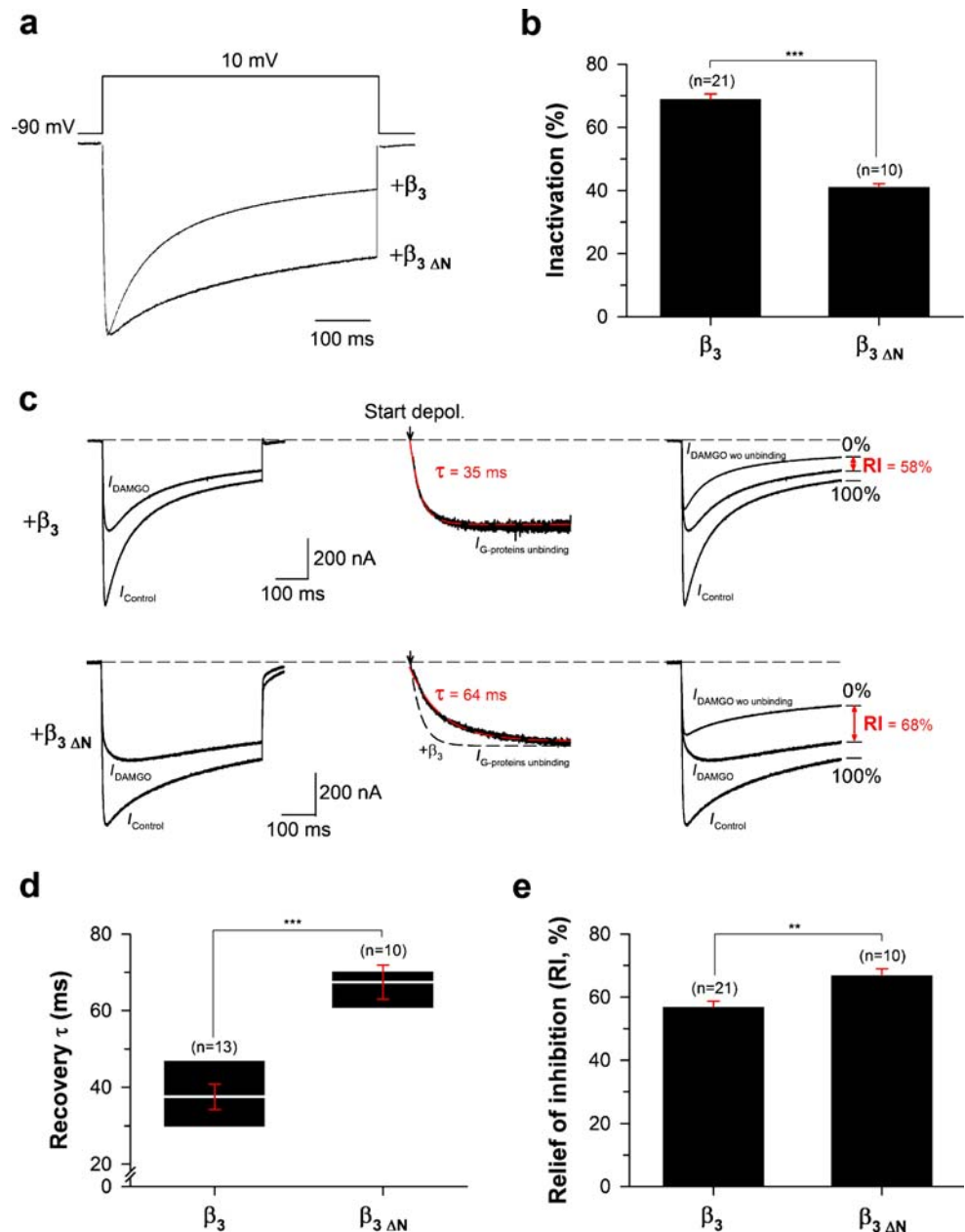
Fig. 4 Slowing of inactivation kinetics by N-terminal truncated β_{1b} subunit modifies the recovery of N-type current inhibition by G-proteins. **a** Representative current elicited by a step depolarization at 10 mV for $\text{Ca}_v2.2$ channels co-expressed with the wild-type β_{1b} subunit or with the N-terminal truncated subunit. Current traces were normalized to facilitate comparison of the kinetics and extent of inactivation. **b** Block diagram representation of the extent of inactivated current after 500 ms depolarization. **c** Representative current traces before (I_{Control}) and during application of 10 μM DAMGO (I_{DAMGO}) are shown at 10 mV for $\text{Ca}_v2.2$ channels co-expressed with the wild-type β_{1b} subunit or with the truncated subunit (left panel). Corresponding normalized $I_{\text{G-protein unbinding}}$ traces fitted by a mono-exponential decrease (red dashed line) are shown for each condition (middle panel). The arrow indicates the start of the depolarization. The black dotted line represents the $\text{Ca}_v2.2/\beta_{1b}$ channel condition shown for comparison. Corresponding traces, which allowed the measure of RI values (in red), are also shown for each experimental condition (right panel). **d** Box plot representation of time constants τ of recovery from G-protein inhibition at 10 mV for each experimental condition. **e** Block diagram representation of RI values after 500 ms depolarization at 10 mV for each experimental condition. Data are expressed as mean \pm SEM (in red) for n studied cells. Statistical t test: three asterisks denote $p \leq 0.001$



potentials (Fig. 7a, right panel). This τ value was chosen because it allows the incorporation of a large number of recordings in the analysis. Also, with a τ of 50 ms, the RI value at 500 ms after depolarization has reached saturation (95% of recovery after 150 ms of depolarization). For traces that underwent a recovery from inhibition with a τ value of 50 ± 5 ms, we measured the extent of RI and of inactivation, both at 500 ms. Representative examples for different channel combinations ($\text{Ca}_v2.2$ along with either β_{2a} , β_4 , or β_{1b} from the slowest to the fastest inactivation) are shown in Fig. 7b (left panel) where the RI values and the extent of inactivation (right panel) are measured in each experi-

mental condition. Figure 7c shows the negative correlation existing between the extent of maximum recovery from inhibition and the extent of inactivation (statistically significant at $p < 0.001$, $n=62$). These results demonstrate that the only restriction to observe a complete current recovery from G-protein inhibition is the inactivation process. Indeed, channels that have almost no inactivation ($\text{Ca}_v2.2/\beta_{2a}$) show a complete recovery from inhibition. The curve predicts that, for completely non-inactivating channels, 100% of the current would recover from inhibition. These results confirm that the experimental protocol used herein to minimize voltage-independent

Fig. 5 Slower inactivation kinetics induced by N-terminal truncated β_3 subunit also modifies recovery of N-type current inhibition by G-proteins. Legends as in Fig. 4 but for cells expressing $\text{Ca}_v2.2$ channels in combination with the wild-type β_3 subunit or with the N-terminal truncated subunit. Data are expressed as mean \pm SEM (in red) for n studied cells. Statistical t test: two asterisks denote $p \leq 0.01$, while three asterisks denote $p \leq 0.001$



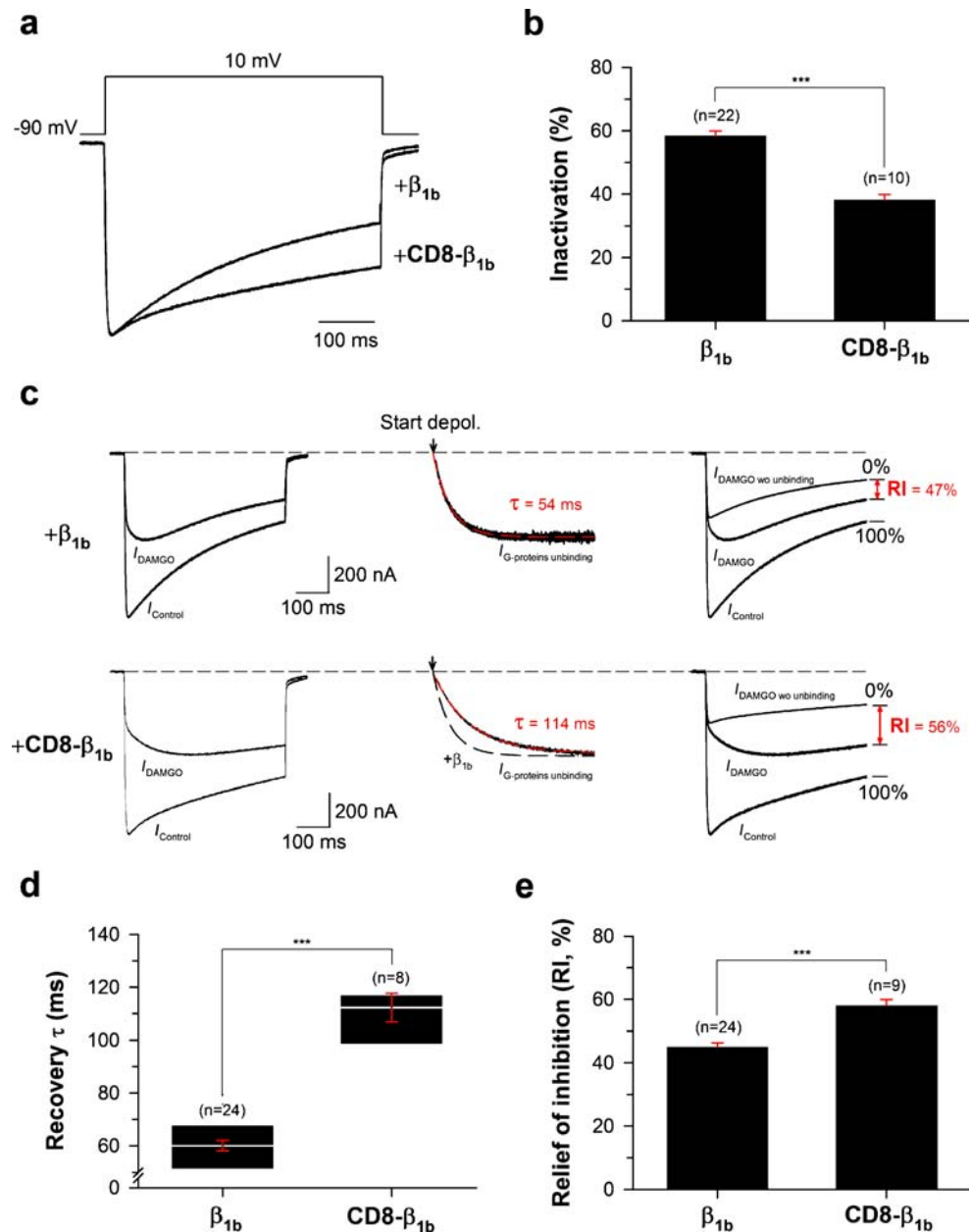
inhibition was fully functional. Conversely, channels that present the most inactivation present the smallest amount of recovery from inhibition.

Differences in calcium channel inactivation generate drastic differences in the biophysical characteristics of G-protein regulation

Since recovery from G-protein inhibition induces an apparent slowing of activation and inactivation kinetics, and shifts the voltage dependence of activation towards depolarized values [49], differences in channel inactivation that affect the recovery process should also affect the

biophysical effects of G-proteins on N-type channels. Calcium currents are generally measured at peak amplitudes. The consequences of this protocol are shown for $\text{Ca}_v2.2/\beta_{1b}$ and $\text{Ca}_v2.2/\beta_{1b\Delta N}$ channels that present different inactivation kinetics (Fig. 8a,b). Several observations can be raised. First, it is observed that the slowing of the $\text{Ca}_v2.2$ inactivation induced by truncating the N terminus of β_{1b} is responsible for a drastic slowing of activation kinetics under DAMGO application. This effect is most pronounced at low potential values and is significantly reduced at high potential values. These effects are quantified in Fig. 8c. For instance, at 0 mV, the average shift of the time to peak for $\text{Ca}_v2.2/\beta_{1b\Delta N}$ channels ($307.7 \pm$

Fig. 6 Slowing of inactivation kinetics by membrane anchoring of β_{1b} subunit modifies recovery of N-type current inhibition by G-proteins. Legends as in Fig. 4 but for cells expressing $\text{Ca}_v2.2$ channels in combination with the wild-type β_{1b} subunit or with the membrane-linked CD8- β_{1b} subunit. Data are expressed as mean \pm SEM (in red) for n studied cells. Statistical t test: three asterisks denote $p \leq 0.001$



9.0 ms, $n=10$) is, on average, 9.2-fold greater than that observed for $\text{Ca}_v2.2/\beta_{1b}$ channels (33.4 ± 5.2 ms, $n=19$; Fig. 8c). Differences in slowing of activation kinetics, triggered by the two β subunits, remain statistically significant for potential values up to 30 mV. Above 30 mV, the convergence of both curves can be explained by the fact that recovery from G-protein inhibition becomes too rapid to be influenced by changes in inactivation kinetics. Second, at the time points of the peak of the current, slowing of inactivation by the N-terminal truncation of β_{1b} induces (1) a hyperpolarizing shift of the voltage dependence of RI_{peak} values, and (2) an increase in RI_{peak} values for potentials equal or below 30 mV (Fig. 8d). Since

RI_{peak} values represent a voltage-dependent gain of current that is added to the unblocked fraction of control currents under G-protein regulation, they apparently modify the voltage dependence of channel activation (I/V curves) and reduce the level of DAMGO inhibition [49]. For the $\text{Ca}_v2.2/\beta_{1b}$ channels, the average half-activation potential values were significantly shifted by 6.4 ± 0.9 mV ($n=13$) under DAMGO inhibition, whereas for the $\text{Ca}_v2.2/\beta_{1b} \Delta N$ channels, a nonsignificant shift by 1.9 ± 0.5 mV ($n=10$) was determined (Fig. 8e,f). This difference in behavior can readily be explained by the voltage dependence of RI_{peak} values. In the case of $\text{Ca}_v2.2/\beta_{1b}$, the maximal RI_{peak} occurs at 30 mV (Fig. 8d), a depolarizing shift of 20 mV

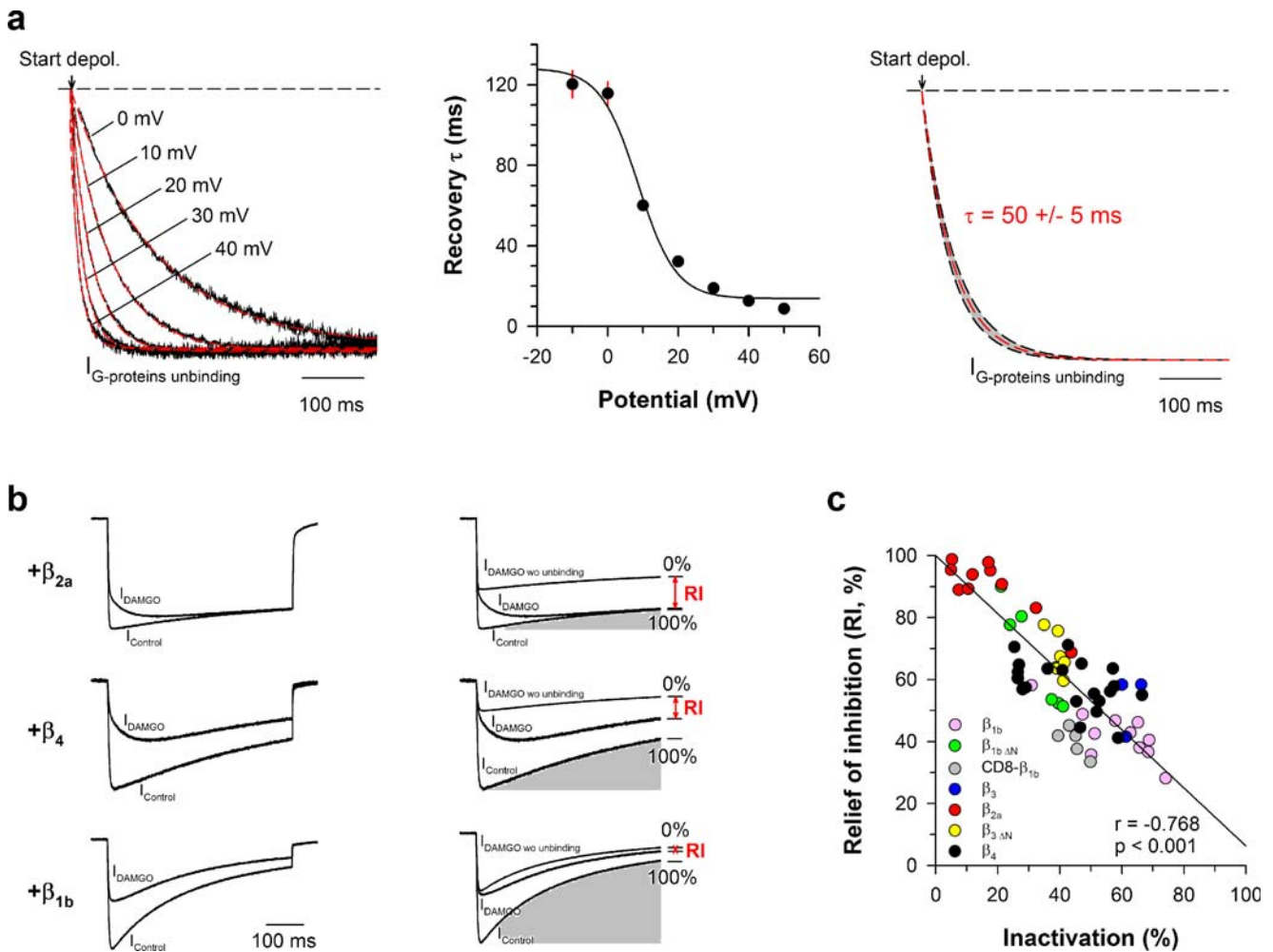


Fig. 7 The extent of N-type channel inactivation correlates with the extent of current recovery from G-protein inhibition. **a** An example of the influence of membrane potential values on the time constant τ of current recovery from G-protein inhibition is shown for $Ca_v2.2/\beta_{1b}$ channels. Normalized $I_{G\text{-protein unbinding}}$ traces fitted by a mono-exponential decrease (red dashed line) are shown for a range of potentials from 0 to +40 mV (left panel). The arrow indicates the start of the depolarization. Traces were superimposed to facilitate kinetic comparisons. Corresponding voltage-dependence of the time constant τ of current recovery from G-protein inhibition ($n=13$) is shown (middle panel). Data are expressed as mean \pm SEM (in red) and were fitted with a sigmoid function. Scheme illustrating normalized $I_{G\text{-protein unbinding}}$ trace for a defined time constant τ of 50 ± 5 ms (red and black lines, respectively; right panel). The gray area represents the accepted variation in τ values ($\pm 10\%$) for the incorporation of current traces in our subsequent analyses. The arrow

indicates the virtual start of the depolarization. **b** Representative normalized current traces before ($I_{Control}$) and under 10 μ M DAMGO application (I_{DAMGO}) for $Ca_v2.2$ expressed in combination with β_{2a} , β_4 , or β_{1b} subunit at +20, +10, and +10 mV, respectively (left panel). Traces were selected on the basis of the measured recovery G-protein inhibition time constant τ (between 45 and 55 ms). Corresponding traces allowing the measurement of RI values (in red) after a 500-ms depolarization (right panel). The gray area represents the extent of current inactivation during a 500-ms depolarization. **c** Scattered plot representation of RI values after a 500-ms depolarization as a function of the extent of inactivation. Values are shown for various $Ca_v2.2/\beta$ combinations ($n=62$) showing a time constant τ of recovery from G-protein inhibition of 50 ± 5 ms independently of the test potential. Fitting these values by a linear curve provided a linear regression coefficient of -0.768 , which is statistically significant at $p < 0.001$ (Spearman rank order correlation test)

compared to control $Ca_v2.2/\beta_{1b}$ currents, which is responsible for the depolarizing shift of the I/V curve under DAMGO inhibition (Fig. 8e). Conversely, for $Ca_v2.2/\beta_{1b \Delta N}$, the maximal RI_{peak} value is observed at 10 mV (Fig. 8d), which is -5 mV hyperpolarized to the control $Ca_v2.2/\beta_{1b \Delta N}$ peak currents and, therefore, influences far less the I/V curve under DAMGO inhibition (Fig. 8f). Finally, it should be noted that with a slowing of inactivation kinetics, the resultant increase in RI_{peak} values

(Fig. 8d, for potentials below 40 mV) produces an apparent reduction in DAMGO inhibition that is clearly evident when one compares the effect of DAMGO on I/V curves of $Ca_v2.2/\beta_{1b}$ and $Ca_v2.2/\beta_{1b \Delta N}$ (Fig. 8e,f).

In conclusion, these data indicate that slowing of channel inactivation kinetics increases the slowing of the time to peak by DAMGO, whereas it reduces both the peak current inhibition and the depolarizing shift of the voltage dependence of activation.

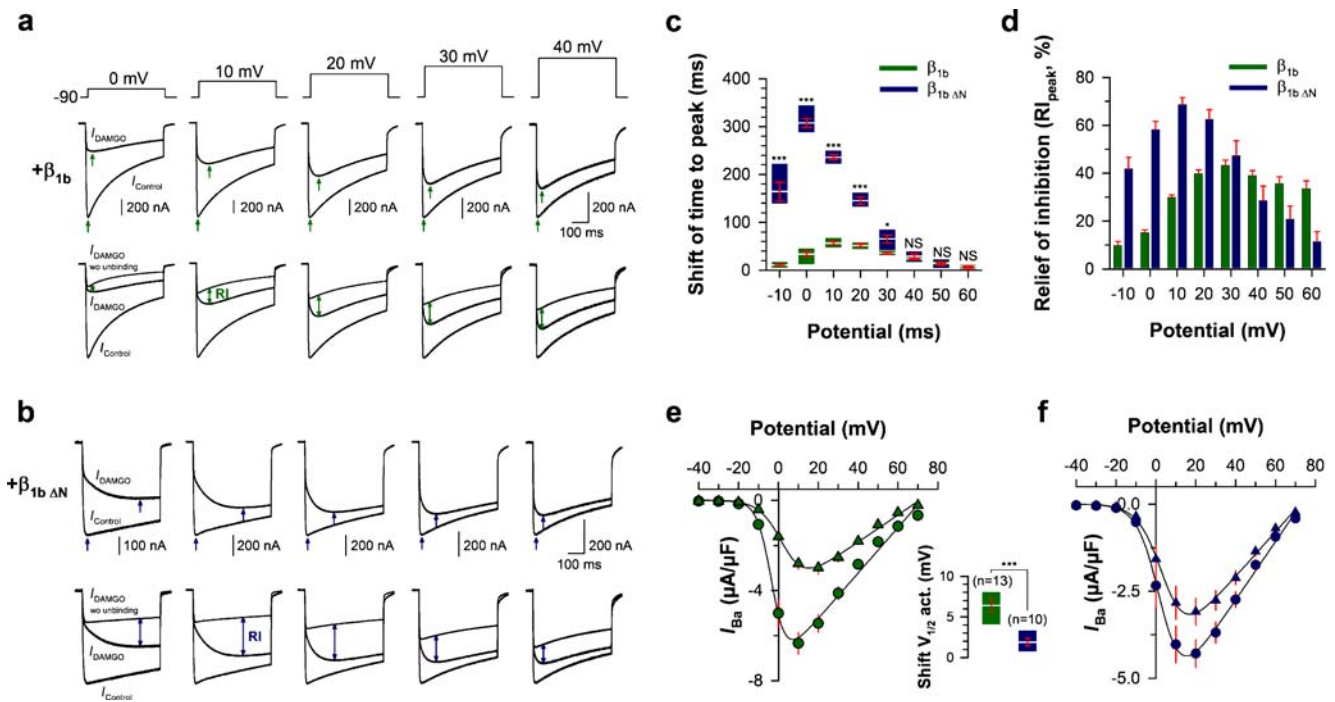


Fig. 8 Effect of channel inactivation on characteristic biophysical changes induced by G-protein activation. Representative current traces before ($I_{Control}$) and under 10 μ M DAMGO application (I_{DAMGO}) and corresponding traces allowing the measurement of RI values are shown for $Ca_v2.2/\beta_{1b}$ (**a**) and $Ca_v2.2/\beta_{1b\Delta N}$ (**b**) at various membrane potentials illustrating DAMGO effects on channel activation kinetics and current recovery from G-protein inhibition in two conditions of channel inactivation. Arrows indicate the time to peak of the currents for control and DAMGO conditions (top panels). The time to peak of DAMGO-inhibited currents (I_{DAMGO}) was also indicated on RI traces (arrows in lower panels). Double arrows indicate the extent of current recovery from G-protein inhibition at these time points (RI_{peak}). **c** Box plot representation of the shift of the current time to peak induced by DAMGO application for $Ca_v2.2/\beta_{1b}$ channels (green boxes, $n=14$) and $Ca_v2.2/\beta_{1b\Delta N}$ channels (blue boxes, $n=10$) as a function of membrane potential. **d** Histogram

representation of RI_{peak} values at the peak of DAMGO currents (I_{DAMGO}) for $Ca_v2.2/\beta_{1b}$ channels (green bars, $n=14$) and $Ca_v2.2/\beta_{1b\Delta N}$ channels (blue bars, $n=10$) as a function of membrane potential. Current–voltage relationship (I/V) were performed for $Ca_v2.2/\beta_{1b}$ channels (green plots, $n=13$; **e**) and $Ca_v2.2/\beta_{1b\Delta N}$ channels (blue plots, $n=10$; **f**) for control (circle symbol) and DAMGO-inhibited (triangle symbols) currents measured at their peak. Data were fitted with a modified Boltzmann equation as described in the “Materials and methods” section. The insert represents the shift of the half-maximum current activation potential ($V_{1/2}$) induced by DAMGO application for $Ca_v2.2/\beta_{1b}$ (green box, $n=13$) and $Ca_v2.2/\beta_{1b\Delta N}$ channels (blue box, $n=10$). Data are expressed as mean \pm SEM (in red) for n studied cells. Statistical t test: NS not statistically significant, single asterisk $p \leq 0.05$, two asterisks $p \leq 0.01$, three asterisks $p \leq 0.001$

Discussion

Relevant parameters to study the influence of inactivation on N-type channel regulation by G-proteins

N-type channel regulation by G-proteins can be described accurately by three parameters: the G-protein inhibition level at the onset of depolarization (GI_0), the time constant of recovery from inhibition (τ), and the maximal extent of recovery from inhibition (RI). GI_0 is indicative of the “ON” effect, whereas τ and RI are the quantitative parameters leading to all “OFF” effects of the G-protein regulation [49]. Since GI_0 is a quantitative index of the extent of G-protein inhibition at the start of the depolarization, i.e., at a time point where no inactivation has yet occurred, inactivation cannot influence this parameter. On the other hand, G-

protein dissociation is a time-dependent process at any given membrane potential and can thus be affected by channel inactivation since both processes occur within a similar timescale. In this study, we aimed at investigating this issue and came up with two novel conclusions. First, channel inactivation kinetics influences the speed of G-protein dissociation, and second, removal of G-proteins occurs within a time window that is closely controlled by inactivation. Hence, the speed of G-protein dissociation and the time window during which this process may occur control the extent of current recovery from G-protein inhibition at any given time. These conclusions were derived from the use of a recent biophysical method of analysis of N-type calcium channel regulation by G-proteins, which is independent of potential changes in channel inactivation behavior while G-proteins are bound onto the channels [48].

G-protein inhibition is completely reversible during depolarization provided that the channel has slow inactivation

There are two physiological ways to terminate direct G-protein regulation on N-type calcium channels: (1) the end of GPCR stimulation by recapture or degradation of the agonist (experimentally mimicked by washout of the bath medium), and (2) membrane depolarization by trains of action potentials (experimentally simulated by a prepulse application). Whereas the first one always leads to a complete recovery from G-protein inhibition, the second one produces a transient and variable recovery. Interestingly, a very slowly inactivating channel, such as the one produced by the combination of $Ca_v2.2$ and β_{2a} subunits, can lead to a complete recovery from G-protein inhibition after membrane depolarization, whereas a fast inactivating channel, such as the one produced by the co-expression of the β_{1b} subunit, leads only to a partial recovery. For slow inactivating channels, the time window for G-protein dissociation is large since channel inactivation does not interfere with the process. Conversely, for fast inactivating channels, the time window for G-proteins to unbind from the channel is considerably reduced since inactivation prevents the observation of a complete recovery from inhibition. For these channels, the extent of recovery from inhibition is controlled by both the speed of G-protein dissociation and the time window of opportunity. Hence, the speed of current recovery from G-protein inhibition is controlled by channel inactivation and by channel opening as previously shown [49], whereas the time window opportunity of this process is only controlled by channel inactivation. It is likely that both parameters (the time constant of recovery τ and the time window of opportunity) are under the control of additional molecular players or channel-modifying agents such as phosphorylation that may act on one or the other parameters in an independent manner, and could contribute to a fine control of the direct G-protein regulation.

There is an unexpected relationship between the channel inactivation kinetics and the kinetics of current recovery from G-protein inhibition

One surprising observation from this study is that fast inactivation accelerates the speed of current recovery from G-protein inhibition, whereas slower inactivation slows down G-protein dissociation from the channel. This was first demonstrated through the use of different β subunit isoforms (see also [12, 20]), and then confirmed with β subunit constructs known to modify channel inactivation kinetics. Besides this functional correlation, there might be a structural basis that underlies a mechanistic link between

channel inactivation and G-protein dissociation. Indeed, Herlitz et al. [23] illustrated that an R to A mutation of the QXXER motif (one of the $G_{\beta\gamma}$ -binding determinant within the I–II linker of $Ca_v2.x$ channels [15]) slows both the inactivation kinetics and the recovery from G-protein inhibition. The I–II loop of $Ca_v2.2$ appears as a particularly interesting structural determinant for supporting G-protein dissociation. First, it contains several $G_{\beta\gamma}$ -binding determinants whose functional role remain unclear [11, 15, 23, 33, 53, 54]. Second, this loop is known to contribute to fast inactivation [21, 23, 46]) possibly through a hinged lid mechanism that would impede the ion pore [46]. Third, some of the residues of the QXXER motif have been found to contribute to inactivation in a voltage-sensitive manner [41]. A possible working hypothesis for the contribution of the I–II loop to G-protein regulation can be proposed: (1) the channel openings provide an initial destabilizing event favoring G-protein dissociation, and (2) the hinged lid movement of the I–II loop triggered by the inactivation process further accelerates G-protein dissociation through an additional decrease in affinity between $G_{\beta\gamma}$ and the channel.

However, there is an alternative possibility based on the expected relationship between channel opening probability and rate of G-protein dissociation [49]. At the potential at which we performed this study (10 mV), all channel combinations are at their maximal activation (data not shown) and should produce maximal opening probabilities. Nevertheless, we cannot rule out that the various β subunits and structural analogues introduce differences in the maximal opening probabilities of the channel thereby explaining differences in the rate of G protein dissociation, e.g., β_{2a} with a lower opening probability and, thus, slower recovery from inhibition. However, this would imply that anything that leads to a slowing of inactivation kinetics, through a modification of β subunit structure, produces a reduced opening probability. The likelihood of this hypothesis is probably low, but cannot be dismissed.

Inactivation differentially affects each characteristic biophysical channel modification induced during G-protein regulation

Since time-dependent G-protein dissociation is responsible for the characteristic biophysical modifications of the channel [49], inactivation, by altering the parameters of the recovery from inhibition, plays a crucial role in the phenotype of G-protein regulation. Two extreme case scenarios were observed. G-protein regulation of slowly inactivating channels, such as $Ca_v2.2/\beta_{1b \Delta N}$, induces an important slowing of the activation kinetics, but no or little depolarizing shift of the voltage dependence of activation and less peak current inhibition. Conversely, faster inacti-

vating channels, such as $\text{Ca}_v2.2/\beta_{1b}$, present reduced slowing of activation kinetics, but a greater peak current inhibition and a marked depolarizing shift of the voltage dependence of activation. These data point to the fact that characteristic biophysical changes of the channel under G-protein regulation should not be correlated with each other. Indeed, an important shift of the time to peak is not necessarily associated with an important depolarizing shift of the voltage dependence of activation or a greater peak current reduction. Thus, it seems important to be cautious on the absence of a particular phenotype of G-protein regulation that does not necessarily reflect the lack of direct G-protein inhibition.

Physiological implications of channel inactivation in G-protein regulation

N-type channels are rather heterogeneous by their inactivation properties because of differences in subunit composition [43] or in alternative splicing [5, 28]. Very little information is available on the targeting determinants that lead to N-type channel insertion at the synapse. However, a contribution of the β subunits and of specific C-terminal sequences of $\text{Ca}_v2.2$ is thought to be involved in the sorting of mature channels [24]. An epileptic lethargic phenotype in mouse is known to arise from the loss of expression of the β_4 subunit, which is accompanied by a β -subunit reshuffling in the N-type channels [9]. These animals present an altered excitatory synaptic transmission suggesting the occurrence of a modification in channel composition and/or regulation at the synapse [10]. Synaptic terminals that arise from single axons present a surprising heterogeneity in calcium channel composition and in processing capabilities [39]. One of the synaptic properties most influenced by calcium channel subtypes is presynaptic inhibition by G-proteins. Evidence has been provided that the extent of N-type current facilitation (hence, current recovery from G-protein inhibition) is dependent on both the duration [8] and the frequency of action potentials (AP) [36, 50]. Low frequencies of AP produce no or little recovery, whereas high-frequency action potentials more dramatically enhance recovery. Hence, slowly inactivating channels should allow much better recovery from G-protein inhibition than fastly inactivating channels, thereby further enhancing the processing abilities of synaptic terminals. In that sense, a model of synaptic integration has been proposed by the group of Dr. Zamponi [6] that would be implicated in short-term synaptic facilitation or depression. It should be noted that the inactivation of calcium channels does not only rely on a voltage-dependent component and that other modulatory signals (calcium-dependent inactivation, phosphorylation) need to find a place in the integration pathway.

Conclusion

These data permit a better understanding of the role of inactivation in N-type calcium channel regulation by G-proteins and will call attention to the contribution of the different β subunits in physiological responses at the synapse.

Acknowledgements We thank Dr. Pierre Charnet and Dr. Yasuo Mori for providing the cDNAs encoding the rat μ -opioid receptor and the rabbit $\text{Ca}_v2.2$ channel, respectively. We are indebted to Dr. Anne Feltz, Dr. Lubica Lacinova, Dr. Michel Vivaudou, and Dr. Eric Hosity for critical evaluation of this work. We thank Sandrine Geib for her contribution to the $\text{CD8-}\beta_{1b}$ construct.

References

1. Agler HL, Evans J, Tay LH, Anderson MJ, Colecraft HM, Yue DT (2005) G protein-gated inhibitory module of N-type ($\text{Ca}_v2.2$) Ca^{2+} channels. *Neuron* 46:891–904
2. Ahern CA, Sheridan DC, Cheng W, Mortenson L, Nataraj P, Allen P, De Waard M, Coronado R (2003) Ca^{2+} current and charge movements in skeletal myotubes promoted by the β -subunit of the dihydropyridine receptor in the absence of ryanodine receptor type 1. *Biophys J* 84:942–959
3. Artalejo CR, Adams ME, Fox AP (1994) Three types of Ca^{2+} channel trigger secretion with different efficacies in chromaffin cells. *Nature* 367:72–76
4. Bean BP (1989) Neurotransmitter inhibition of neuronal calcium currents by changes in channel voltage dependence. *Nature* 340:153–156
5. Bell TJ, Thaler C, Castiglioni AJ, Helton TD, Lipscombe D (2004) Cell-specific alternative splicing increases calcium channel current density in the pain pathway. *Neuron* 41:127–138
6. Bertram R, Swanson J, Yousef M, Feng ZP, Zamponi GW (2003) A minimal model for G protein-mediated synaptic facilitation and depression. *J Neurophysiol* 90:1643–1653
7. Boland LM, Bean BP (1993) Modulation of N-type calcium channels in bullfrog sympathetic neurons by luteinizing hormone-releasing hormone: kinetics and voltage dependence. *J Neurosci* 13:516–533
8. Brody DL, Patil PG, Mulle JG, Snutch TP, Yue DT (1997) Bursts of action potential waveforms relieve G-protein inhibition of recombinant P/Q-type Ca^{2+} channels in HEK 293 cells. *J Physiol* 499(Pt 3):637–644
9. Burgess DL, Jones JM, Meisler MH, Noebels JL (1997) Mutation of the Ca^{2+} channel β subunit gene *Cchb4* is associated with ataxia and seizures in the lethargic (lh) mouse. *Cell* 88:385–392
10. Caddick SJ, Wang C, Fletcher CF, Jenkins NA, Copeland NG, Hosford DA (1999) Excitatory but not inhibitory synaptic transmission is reduced in lethargic (*Cacnb4(lh)*) and tottering (*Caen1atg*) mouse thalami. *J Neurophysiol* 81:2066–2074
11. Canti C, Page KM, Stephens GJ, Dolphin AC (1999) Identification of residues in the N terminus of α_{1B} critical for inhibition of the voltage-dependent calcium channel by $G_{\beta\gamma}$. *J Neurosci* 19:6855–6864
12. Canti C, Bogdanov Y, Dolphin AC (2000) Interaction between G proteins and accessory subunits in the regulation of α_{1B} calcium channels in *Xenopus* oocytes. *J Physiol* 527(Pt 3):419–432
13. Chien AJ, Carr KM, Shirokov RE, Rios E, Hosey MM (1996) Identification of palmitoylation sites within the L-type calcium

- channel β_{2a} subunit and effects on channel function. *J Biol Chem* 271:26465–26468
14. De Waard M, Pragnell M, Campbell KP (1994) Ca^{2+} channel regulation by a conserved β subunit domain. *Neuron* 13:495–503
 15. De Waard M, Liu H, Walker D, Scott VE, Gurnett CA, Campbell KP (1997) Direct binding of G-protein $\beta\gamma$ complex to voltage-dependent calcium channels. *Nature* 385:446–450
 16. De Waard M, Hering J, Weiss N, Feltz A (2005) How do G proteins directly control neuronal Ca^{2+} channel function? *Trends Pharmacol Sci* 26:427–436
 17. Doupnik CA, Pun RY (1994) G-protein activation mediates prepulse facilitation of Ca^{2+} channel currents in bovine chromaffin cells. *J Membr Biol* 140:47–56
 18. Dunlap K, Fischbach GD (1981) Neurotransmitters decrease the calcium conductance activated by depolarization of embryonic chick sensory neurones. *J Physiol* 317:519–535
 19. Eppig JJ, Dumont JN (1976) Defined nutrient medium for the in vitro maintenance of *Xenopus laevis* oocytes. *In Vitro* 12:418–427
 20. Feng ZP, Amot MI, Doering CJ, Zamponi GW (2001) Calcium channel β subunits differentially regulate the inhibition of N-type channels by individual G_{β} isoforms. *J Biol Chem* 276:45051–45058
 21. Geib S, Sandoz G, Cornet V, Mabrouk K, Fund-Saunier O, Bichet D, Villaz M, Hoshi T, Sabatier JM, De Waard M (2002) The interaction between the I–II loop and the III–IV loop of $\text{Ca}_v2.1$ contributes to voltage-dependent inactivation in a β -dependent manner. *J Biol Chem* 277:10003–10013
 22. Herlitze S, Garcia DE, Mackie K, Hille B, Scheuer T, Catterall WA (1996) Modulation of Ca^{2+} channels by G-protein $\beta\gamma$ subunits. *Nature* 380:258–262
 23. Herlitze S, Hockerman GH, Scheuer T, Catterall WA (1997) Molecular determinants of inactivation and G protein modulation in the intracellular loop connecting domains I and II of the calcium channel α_{1A} subunit. *Proc Natl Acad Sci USA* 94:1512–1516
 24. Herlitze S, Xie M, Han J, Hummer A, Melnik-Martinez KV, Moreno RL, Mark MD (2003) Targeting mechanisms of high voltage-activated Ca^{2+} channels. *J Bioenerg Biomembr* 35:621–637
 25. Hille B (1994) Modulation of ion-channel function by G-protein-coupled receptors. *Trends Neurosci* 17:531–536
 26. Ikeda SR (1991) Double-pulse calcium channel current facilitation in adult rat sympathetic neurones. *J Physiol* 439:181–214
 27. Ikeda SR (1996) Voltage-dependent modulation of N-type calcium channels by G-protein $\beta\gamma$ subunits. *Nature* 380:255–258
 28. Lin Z, Haus S, Edgerton J, Lipscombe D (1997) Identification of functionally distinct isoforms of the N-type Ca^{2+} channel in rat sympathetic ganglia and brain. *Neuron* 18:153–166
 29. Lipscombe D, Kongsamut S, Tsien RW (1989) α -adrenergic inhibition of sympathetic neurotransmitter release mediated by modulation of N-type calcium-channel gating. *Nature* 340:639–642
 30. Marchetti C, Carbone E, Lux HD (1986) Effects of dopamine and noradrenaline on Ca^{2+} channels of cultured sensory and sympathetic neurons of chick. *Pflugers Arch* 406:104–111
 31. Meir A, Dolphin AC (2002) Kinetics and $G_{\beta\gamma}$ modulation of $\text{Ca}_v2.2$ channels with different auxiliary β subunits. *Pflugers Arch* 444:263–275
 32. Olcese R, Qin N, Schneider T, Neely A, Wei X, Stefani E, Birnbaumer L (1994) The amino terminus of a calcium channel β subunit sets rates of channel inactivation independently of the subunit's effect on activation. *Neuron* 13:1433–1438
 33. Page KM, Stephens GJ, Berrow NS, Dolphin AC (1997) The intracellular loop between domains I and II of the B-type calcium channel confers aspects of G-protein sensitivity to the E-type calcium channel. *J Neurosci* 17:1330–1338
 34. Page KM, Canti C, Stephens GJ, Berrow NS, Dolphin AC (1998) Identification of the amino terminus of neuronal Ca^{2+} channel α_1 subunits α_{1B} and α_{1E} as an essential determinant of G-protein modulation. *J Neurosci* 18:4815–4824
 35. Patil PG, de Leon M, Reed RR, Dubel S, Snutch TP, Yue DT (1996) Elementary events underlying voltage-dependent G-protein inhibition of N-type calcium channels. *Biophys J* 71:2509–2521
 36. Penington NJ, Kelly JS, Fox AP (1991) A study of the mechanism of Ca^{2+} current inhibition produced by serotonin in rat dorsal raphe neurons. *J Neurosci* 11:3594–3609
 37. Qin N, Olcese R, Zhou J, Cabello OA, Birnbaumer L, Stefani E (1996) Identification of a second region of the β -subunit involved in regulation of calcium channel inactivation. *Am J Physiol* 271: C1539–C1545
 38. Qin N, Platano D, Olcese R, Stefani E, Birnbaumer L (1997) Direct interaction of $G_{\beta\gamma}$ with a C-terminal $G_{\beta\gamma}$ -binding domain of the Ca^{2+} channel α_1 subunit is responsible for channel inhibition by G protein-coupled receptors. *Proc Natl Acad Sci USA* 94:8866–8871
 39. Reid CA, Bekkers JM, Clements JD (2003) Presynaptic Ca^{2+} channels: a functional patchwork. *Trends Neurosci* 26:683–687
 40. Restituito S, Cens T, Barrere C, Geib S, Galas S, De Waard M, Charnet P (2000) The β_{2a} subunit is a molecular groom for the Ca^{2+} channel inactivation gate. *J Neurosci* 20:9046–9052
 41. Sandoz G, Lopez-Gonzalez I, Stambouliau S, Weiss N, Amoult C, De Waard M (2004) Repositioning of charged I–II loop amino acid residues within the electric field by β subunit as a novel working hypothesis for the control of fast P/Q calcium channel inactivation. *Eur J Neurosci* 19:1759–1772
 42. Scott RH, Dolphin AC (1990) Voltage-dependent modulation of rat sensory neurone calcium channel currents by G protein activation: effect of a dihydropyridine antagonist. *Br J Pharmacol* 99:629–630
 43. Scott VE, De Waard M, Liu H, Gurnett CA, Venzke DP, Lennon VA, Campbell KP (1996) β subunit heterogeneity in N-type Ca^{2+} channels. *J Biol Chem* 271:3207–3212
 44. Simen AA, Lee CC, Simen BB, Bindokas VP, Miller RJ (2001) The C terminus of the Ca^{2+} channel α_{1B} subunit mediates selective inhibition by G-protein-coupled receptors. *J Neurosci* 21:7587–7597
 45. Stephens GJ, Page KM, Bogdanov Y, Dolphin AC (2000) The α_{1B} Ca^{2+} channel amino terminus contributes determinants for β subunit-mediated voltage-dependent inactivation properties. *J Physiol* 525(Pt 2):377–390
 46. Stotz SC, Hamid J, Spaetgens RL, Jarvis SE, Zamponi GW (2000) Fast inactivation of voltage-dependent calcium channels. A hinged-lid mechanism? *J Biol Chem* 275:24575–24582
 47. Takahashi T, Momiyama A (1993) Different types of calcium channels mediate central synaptic transmission. *Nature* 366:156–158
 48. Weiss N, De Waard M (2006) Introducing an alternative biophysical method to analyze direct G protein regulation of voltage-dependent calcium channels. *J Neurosci Methods*. DOI 10.1016/j.jneumeth.2006.08.010
 49. Weiss N, Amoult C, Feltz A, De Waard M (2006) Contribution of the kinetics of G protein dissociation to the characteristic modifications of N-type calcium channel activity. *Neurosci Res* 56:332–343
 50. Williams S, Serafin M, Muhlethaler M, Bernheim L (1997) Facilitation of N-type calcium current is dependent on the frequency of action potential-like depolarizations in dissociated cholinergic basal forebrain neurons of the guinea pig. *J Neurosci* 17:1625–1632
 51. Wu LG, Saggau P (1997) Presynaptic inhibition of elicited neurotransmitter release. *Trends Neurosci* 20:204–212
 52. Zamponi GW (2001) Determinants of G protein inhibition of presynaptic calcium channels. *Cell Biochem Biophys* 34:79–94
 53. Zamponi GW, Bourinet E, Nelson D, Nargeot J, Snutch TP (1997) Crosstalk between G proteins and protein kinase C mediated by the calcium channel α_1 subunit. *Nature* 385:442–446
 54. Zhang JF, Ellinor PT, Aldrich RW, Tsien RW (1996) Multiple structural elements in voltage-dependent Ca^{2+} channels support their inhibition by G proteins. *Neuron* 17:991–1003